



HAL
open science

Modeling support for nonlinear resonant laser vibrometry: numerical imitation of experiments

Vladislav Aleshin, Ravi Verma, Kevin Truyaert

► **To cite this version:**

Vladislav Aleshin, Ravi Verma, Kevin Truyaert. Modeling support for nonlinear resonant laser vibrometry: numerical imitation of experiments. 16ème Congrès Français d'Acoustique, CFA 2022, Apr 2022, Marseille, France. hal-03653411v2

HAL Id: hal-03653411

<https://hal.science/hal-03653411v2>

Submitted on 27 Apr 2022

HAL is a multi-disciplinary open access archive for the deposit and dissemination of scientific research documents, whether they are published or not. The documents may come from teaching and research institutions in France or abroad, or from public or private research centers.

L'archive ouverte pluridisciplinaire **HAL**, est destinée au dépôt et à la diffusion de documents scientifiques de niveau recherche, publiés ou non, émanant des établissements d'enseignement et de recherche français ou étrangers, des laboratoires publics ou privés.



16^{ème} Congrès Français d'Acoustique
11-15 Avril 2022, Marseille

Modeling support for nonlinear laser vibrometry: numerical imitation of experiments

V. Aleshin ^a, R. Verma ^{a,b} and K. Truyaert ^b

^a IEMN, Université de Lille, France

^b KU Leuven Campus Kortrijk, Belgium



Experimental nonlinear acoustic techniques for visualizing damage in materials and structures have been intensively developing for more than 30 years. It is of interest to supplement them by relevant modeling methods capable of imitating acoustic propagation in damaged materials. The associated gains include the availability of all calculated mechanical fields instead of restrained experimental data, the possibility to predict false detections and false alarms, and, in perspective, to reconstruct real parameters of defects by comparing measured data to synthetic ones. In this work, we model mechanical processes corresponding to laser vibrometry experiments in which nonlinear components of generated acoustic standing waves in a sample approximately reveal the position of damage. To do so, we apply a previously developed numerical method that combines a physical model of frictional contacts representing damage and the finite element formulation for acoustic waves. This physical model accounts for the Coulomb friction law governing mechanics of contacting rough surfaces by using the analogy between rough profiles and axisymmetric contacts of Cattaneo-Mindlin type. The latter ones are successfully described with the help of the original method of memory diagrams capable of calculating contact response to an arbitrary acoustic excitation. In our numerical experiments, we form standing waves in a domain containing a crack with known geometric properties. Depending on structure geometry, excitation type and strength, as well as on damage size, position and depth, we obtain widely different responses containing nonlinear spectral components. We qualitatively compare them to available experimental data and formulate conclusions on theoretical sensitivity of nonlinear resonant methods in various situations.

1 Introduction

This paper is concerned a new method of acoustic modeling in materials with frictional contacts aimed at nondestructive testing (NDT) applications. Frictional contacts are frequency related to damage (cracks, delaminations) in solid structures. Nowadays, contact acoustic nonlinearity is used for detecting positions and extent of damage, at least in laboratory context. It is important to emphasize that nonlinear acoustic NDT is a family of essentially experimental techniques. Numerical models for underlying physical processes exist only in particular cases and on the basis on simplified description of contact nonlinearity. Description of an arbitrary frictional contact excited by an arbitrary acoustic field requires huge computational expenses. The main reason for that is in the fact that the account for friction engenders implicit calculations. The basic approximate model for frictional interaction (Coulomb friction law of $T=\mu N$ type) does not produce the required boundary conditions as a direct link between stresses and displacements. It just says that particular contact fragment can be found in the state of slick or of slip, and defines conditions for that in terms of stresses. The displacements in this case should be adjusted altogether and multiple times in order to satisfy those conditions. In addition, friction makes the problem hysteretic i.e. a current response of a frictional system is not instantaneous but depends on loading history.

Nevertheless, there exists a family of numerical contact mechanics methods [1,2] that successfully address those issues. However, they are typically applied to simple loading histories (e.g. loading-unloading-reloading) whereas acoustic signal contain large number of oscillations. There also exist numerical acoustic methods [3,4,5] applicable to ultrasound signals in the presence of inner frictional contacts but their use is associated with considerable computational expenses coming from an implicit nature of solution.

In a series of publications [6,7,8] it is suggested an alternative approach based on the Cattaneo-Mindlin [9] (also called Hertz-Mindlin [10]) solution. This classical

result links forces and displacements for contact of two spheres loaded by one of a certain set of particular protocols. More recently, two important advances have been suggested: account for non-spherical but axisymmetric shapes [14], and applicability to arbitrary loading histories/protocols [6,7,8]. These methods can be called semi-analytical since the solution remains cumbersome but analytical, and has coefficients determined by an algorithm. In addition, there exist arguments proving that fragments of isotropically rough surfaces in contact interact in the sense of load-displacement relationships in the same way as axisymmetric bodies of appropriate shapes. The semi-analytical methods of this kind provide the sought-for load-displacement relationship in an explicit form that dramatically reduces the calculation effort in comparison with implicit schemes.

Our original method (Method of Memory Diagram, MMD [6,8]) belonging to this group uses internal memory functions or diagrams in which the coefficients of the analytical solutions are encoded. Further, based on those principles, we have developed a so called MMD-FEM numerical tool [11] that describes wave propagation in a material with frictional cracks including nonlinear effects coming from contact interactions. In this paper, we apply the corresponding code to solving a wave problem that underlies an existing nonlinear acoustic imaging technique that uses harmonic content in standing waves generated in a sample by a continuous sinewave excitation. Purely harmonic, the standing wave becomes slightly nonlinear if defects are present. Spatial distribution of the nonlinear wave component can approximately indicate positions and extents of hidden cracks. This technique, the nonlinear resonant laser vibrometry [12], is relatively easy to imitate numerically since it does not require sharp focusing of acoustic waves as other methods do.

In this paper, we briefly explain how the MMD-FEM functions in the considered case and present a number of synthetic nonlinear acoustic images of hidden plane cracks of certain size. These images are shown in a variety of cases determined by geometric and physical parameters of the sample and of the excitation. In addition, the MMD algorithm has an important parameter related to roughness

of crack faces. The influence of these factors is illustrated by numerous examples.

2 Method of memory diagrams

As mentioned above, the MMD is analytical with coefficients “ciphered” in internal memory functions (or diagrams) that are continuously being updated following changes in the loading protocol. The details can be found in [6,8] and include the formulation of the method for partial slip of axisymmetric bodies in contact, and then the generalization of the method for the case of total sliding. As a result, for any sequence of contact states (partial slip, full sliding and contact loss), the solution is expressed in a closed form denoted here as

$$T = T_{MMD}(b(t), a(t)), N = N(a). \quad (1)$$

Here a and b are normal and tangential contact displacements that depend on time, while N and T are normal and tangential forces. In the considered 2D case the force and displacement vectors always stay in one plane.

Here the normal dependence $N=N(a)$ is considered as known. Paper [13] explains why a model form

$$N(a) = C^2 a^2 \quad (2)$$

is appropriate as an approximation arising from several assumption related to rough surface contact mechanics. The authors of [15] have arrived to the same conclusion on the basis of acoustic measurements of the load-force displacement. Their estimate for constant C obtained for two aluminum blocks is used here as an approximate value. Inner cracks can have roughness largely different from the available case, therefore in this work we consider other possible values as well.

Figure 1 illustrates the MMD load-displacement response to an exemplar loading history in terms of the normal and tangential displacement. The automated calculations for hysteretic shapes of the similar kind provide boundary conditions for the wave propagation problem at each discretization point at crack faces (actually, pairs of points located at the opposite faces).

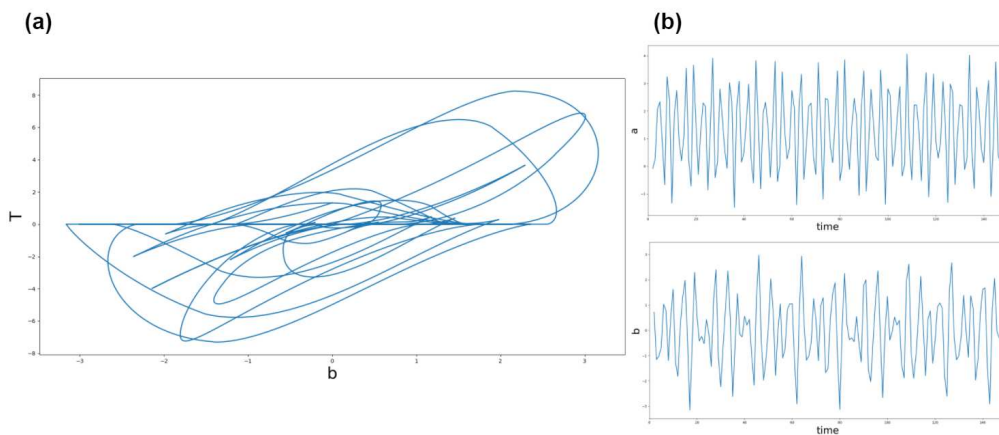


Figure 1 – Hysteretic tangential load-displacement response (a) plotted for exemplar loading history in terms of displacements (b).

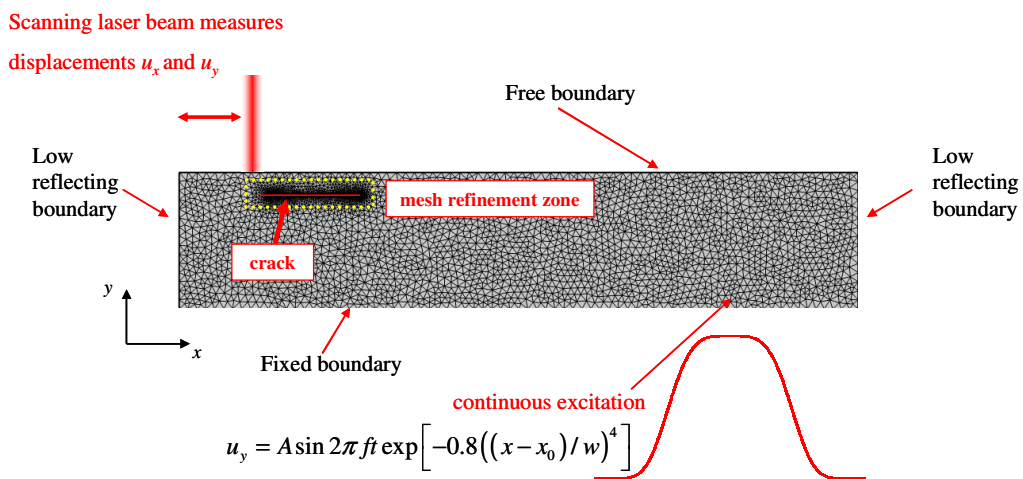


Figure 2 – Geometry of the problem, boundary conditions and excitation type.

3 Geometry of imitated laser vibrometry experiment

It is important to note that numerical acoustics remains time consuming as far as the wave equation itself is concerned. In our examples, several milliseconds of modeled acoustic experiment correspond to hours of calculations. To keep this ratio reasonable, we had to accept two principal simplifications: restrained geometry consisting in a 2D rectangle containing crack, and high values of viscous losses in the material, realistic for composite materials but highly exaggerated for metals or ceramics. The increased viscosity considerably shortens time needed for formation of a stationary solution in the form of a standing wave those amplitude and shape do not depend on time anymore. In addition, the bulk and shear viscosities are considered equal, since their values have an approximate character anyway.

Geometry of the problem and boundary conditions are shown in Figure 2 together with information about excitation. Low reflecting boundaries at the left and right correspond to the case of a fragment of a realistic plate with high geometric aspect ratio. In addition, acoustic energy can effectively go away from the edges acting as additional damping that also shortens the standing wave formation time. Further, to comply with vibrometric experiments, the top surface is considered free; the corresponding displacements are measured by laser beam in reality and are used for the harmonic analysis. In contrast, the bottom surface is fixed. This is important since some boundary conditions should be of the first type (known displacement), otherwise an acoustic action will generate an unlimited motion of the entire plate in free space. Besides, fixing the bottom instead of the left and/or right edges helps prevent bending or cantilever motions that can be excited by low frequencies but are out of interest here. In real laboratory experiments, a plate can be suspended by elastic strings which are difficult to model here since we consider a small fragment only.

The sample is excited by a sinusoidal vertical displacement as shown in the figure. The excitation zone corresponds to an attached transducer and is limited by a supergaussian window.

The crack is located in top left corner. Since it represents a critical element of geometry, mesh is refined around it.

4 Results and discussion

The MMD-FEM code allows one to compute acoustic fields in the sample depicted in Figure 2. The following characteristics are of special interest: wave displacements u_x and u_y at the top boundary that are measured by scanning laser in real experiments, and values of the first strain invariant $\varepsilon_{xx} + \varepsilon_{yy}$ at points close to the transducer and to the crack. The magnitude close to the transducer characterizes the input level signal; generally, values of about 10^{-7} are considered as weak, 10^{-6} typical, and 10^{-5} very strong. Here it is appropriate to cite a known result [16] for the critical tensile stress at which crack starts growing:

$$\sigma_0^2 = \frac{\pi EG}{2R(1-\nu^2)}, \quad (3)$$

where G is the surface energy, and E and ν are respectively Young's modulus and Poisson's ratio of the material. Simple estimations show that for a 3 cm diameter crack in aluminum this critical stress corresponds to strain of about $3.4 \cdot 10^{-5}$. To comply with the spirit of nondestructive testing, the strain in material should be less than that value with a margin.

However, the strain invariant is weaker near the crack since the transducer is located at some distance. The ratio between strain invariants close to the crack and close to the transducer depends on excitation frequency f and ranges between a few percents to about 40%. Certainly, this penetration ratio should be high enough to generate a nonlinear signal of substantial level.

The nonlinear signal or criterion we are talking about is introduced as

$$I_{x,y} = \sum_n \left(\frac{A_n^{x,y}}{A_1^{x,y}} \right)^2 \quad (4)$$

where $A_n^{x,y}$ denotes the n -th harmonic in the spectrum of u_x and u_y displacements at the top surface. These nonlinear criteria as functions of x -coordinate at the top boundary represent images of the crack. The definition Eq. (4) corresponds to the one introduced in experimental work [12] in which its typical level is reported to be about 10^{-3} . It is important to note that the fundamental harmonics $A_1^{x,y}$ added in Eq. (4) as a denominator to compensate for the limited penetration effect can be close to zero at some points, as it frequently occur with a standing wave in general. Zeros in the first harmonics will produce huge parasite peaks in the images. To get rid of this, we applied running averaging to $A_1^{x,y}$ in Eq. (4).

In Figure 3 we present results for a large crack of 3 cm size excited with the same randomly chosen frequency $f=240$ kHz and other parameters varied. Generally, even for weak excitation level in the vicinity of the crack its location and size are clearly visible in images. The signal level at the crack and in the excitation zone is characterized by ε_{cra} and ε_{exc} that represent the amplitudes of the first strain invariant $\varepsilon_{xx} + \varepsilon_{yy}$. This figure also illustrates the influence of parameter C of the normal force-displacement relationship Eq. (2). Its value measured in [15] is $C = 6 \cdot 10^{10} Pa^{1/2} m^{-1}$. Higher levels of C correspond to higher levels of nonlinearity as the nonlinear response is directly related to Eq. (2) and on the hysteretic tangential force also linked with the normal one [6,7]. However, this increase or finally image contrast is not directly proportional to C^2 since apparently for rapidly increasing $N(a)$ the actual displacement a becomes smaller.

The nonlinear response Eq (4) also depends on damping (highly exaggerated here); this dependence has to be clarified additionally.

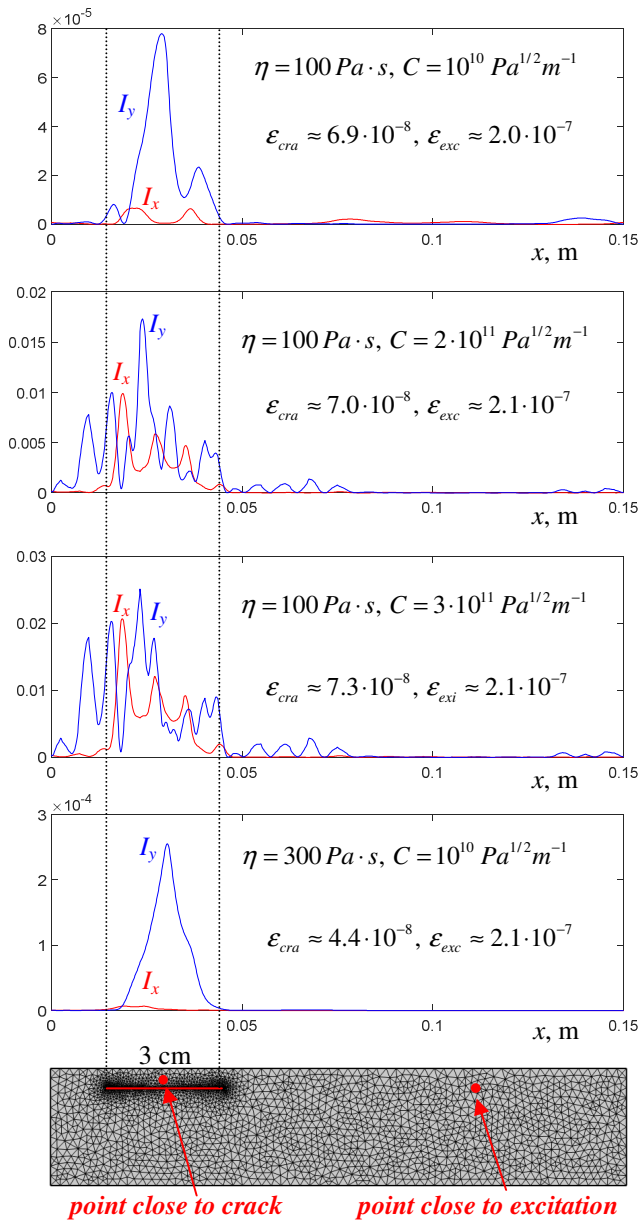


Figure 3 – Nonlinear indicators I_x and I_y calculated for a sample with a crack of 3 cm width excited by a continuous wave of 240 kHz frequency.

The next series of figures (Figure 4) illustrates the effect of frequency on image quality. The nonlinear responses $I_{x,y}$ are calculated for $\eta = 100 \text{ Pa}\cdot\text{s}, C = 10^{10} \text{ Pa}^{1/2}\text{m}^{-1}$ and for a crack size of 2 cm. In all these cases, the excitation displacement amplitude A (see Figure 2) was kept the same.

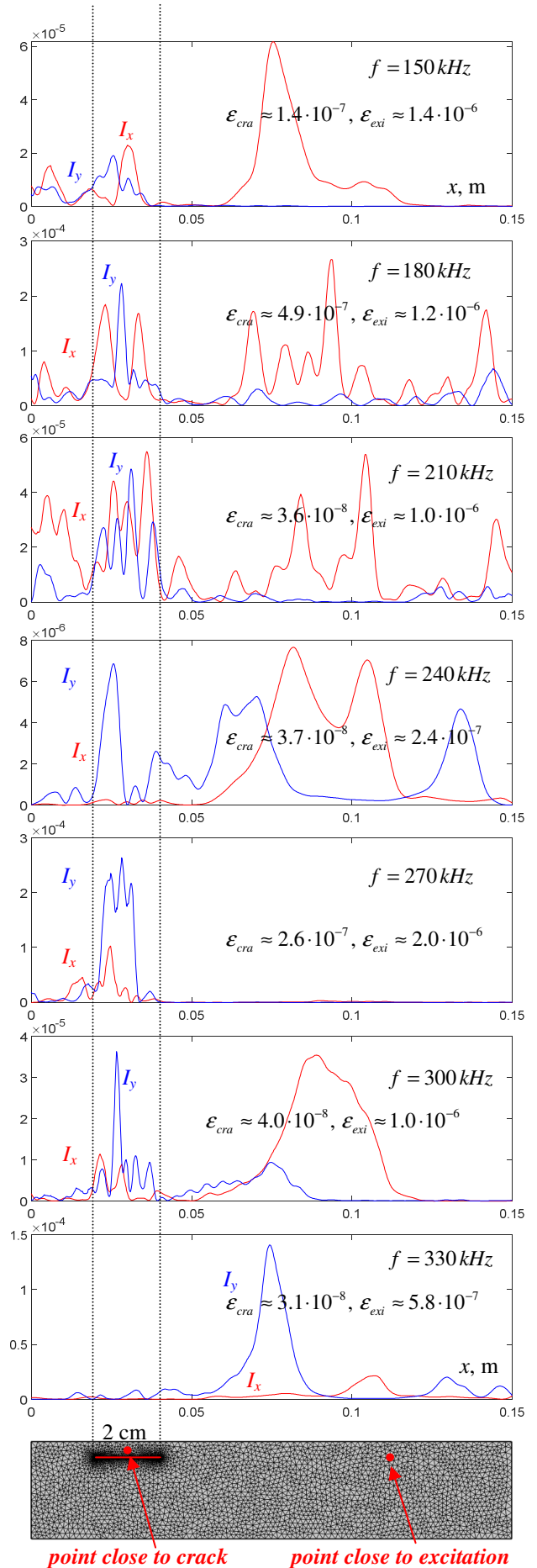


Figure 4 – Nonlinear indicators I_x and I_y calculated for a sample with a crack of 2 cm width excited by a continuous waves of frequencies ranging from 120 to 330 kHz.

First of all, it can be noted that damage is not necessarily seen in all figures. The higher harmonics are not always located near the crack; they have their own standing wave pattern. Certainly, for successful detection it is required to have strong amplitude in the vicinity of crack. It is expected that the idea of local defect resonance [12] can help which consists in finding a specific frequency in the amplitude-frequency response of the sample which exists then damage is present and does not exist otherwise. But even without use of this concept, the choice of frequency is very important since the “penetration ratio” $\varepsilon_{\text{cra}} / \varepsilon_{\text{exc}}$ greatly depends on frequency.

In fact, tendencies that show up in these assorted figures (and in those that remain unpublished) suggest the following strategy of obtaining quality images in which damage is clearly detected.

1. Consider intact sample and examine its amplitude-frequency response by making a series of time-domain calculations or (better) by reconsidering the problem in frequency domain.
2. Select frequencies maximizing the penetration ratio.
3. Choose C less than the value $C = 6 \cdot 10^{10} \text{ Pa}^{1/2} \text{ m}^{-1}$ from [15] since those measurements are done for globally plane aluminum blocks, and real crack faces are rougher. Rough surfaces correspond to smaller C .
4. Make MMD-FEM computations for a cracked sample with selected parameters.

Unfortunately, the problem of damping remains unsolved. Its highly exaggerated value essentially contributes in the nonlinear response. Decreasing damping to smaller and realistic for metals values results in higher times of standing wave formation, whereas the code is now exploited at maximum performance of modern PC.

Certainly, some factors are still not taken into account. For instance, faces of real cracks are typically prestressed. Indeed, once separated during cracking, the faces will not match each other anymore with the atomic precision.

At the same time, we hope that the implementation of the above strategy can help approach real experiments and then validate the entire nonlinear model experimentally. The validated MMD-FEM numerical tool can be an important advance towards modeling-based reconstruction of damage parameters in a better way than pure experimentation can do.

5 Conclusions

In this paper we present the results of numerical modeling for nonlinear laser vibrometry experiments. Using the previously developed MMD-FEM method, we have computed the nonlinear response (sum of higher harmonics amplitudes normalized by the first one) of a sample containing crack with friction. In some cases, damage is

clearly seen in the obtained images and in the others it is not. Our preliminary results allowed one to formulate a possibly strategy for achieving robust damage detection. At the next stage, comparison with experiments is envisaged.

Acknowledgments

R. Verma acknowledges his PhD thesis support by the I-SITE foundation of the University of Lille.

References

- [1] V.A. Yastrebov, Numerical Methods in Contact Mechanics, Wiley-ISTE (2013).
- [2] E.A.H. Vollebregt. User Guide for CONTACT, Rolling and Sliding Contact with Friction (Technical report TR09-03, version 16.1, VORtech BV, Delft, The Netherlands, 2016, www.kalkersoftware.org)
- [3] P. Blanloeuil, A. Meziane, C. Bacon, Numerical study of nonlinear interaction between a crack and elastic waves under an oblique incidence, *Wave Motion* 51 (3) 425–437 (2014).
- [4] P. Blanloeuil, A. Meziane, C. Bacon, 2d finite element modeling of non-collinear mixing method for detection and characterization of closed cracks, *NDT&E Int.* 76, 43–51 (2015).
- [5] P. Blanloeuil, A. Meziane, A. Norris, C. Bacon, Analytical extension of Finite Element solution for computing the nonlinear far field of ultrasonic wavesscattered by a closed crack, *Wave Motion* 66, 132–146 (2016).
- [6] V. Aleshin, O. Bou Matar, K. Van Den Abeele, Method of memory diagrams for mechanical frictional contacts subject to arbitrary 2D loading, *Int. J. Solids Struct.* 60-61, 84–95 (2015).
- [7] V. Popov, M. Hess, Method of Dimensionality Reduction in Contact Mechanics and Friction, Springer Heidelberg New York Dordrecht London (2015).
- [8] V.V. Aleshin, S. Delrue, O. Bou Matar, K. Van Den Abeele, Two dimensional modeling of elastic wave propagation in solids containing cracks with rough surfaces and friction - Part I: Theoretical background. *Ultrasonics* 82, 11-18 (2018).
- [9] C. Cattaneo, Sul contatto di due corpi elastici: distribuzione locale degli sforzi. *Accad. Lincei Rend.* 27(6), 342–348 (1938).
- [10] R. Mindlin, H. Deresiewicz, Elastic spheres in contact under varying oblique forces, *J. Appl. Mech.* 20, 327–344 (1953).
- [11] S. Delrue, V.V. Aleshin, K. Truyaert, O. Bou Matar, K. Van Den Abeele, Two dimensional modeling of elastic wave propagation in solids containing cracks with rough surfaces and friction – Part II: Numerical implementation, *Ultrasonics* 82, 19-30 (2018).
- [12] Kyung-Young Jhang, C.J. Lissenden, I. Solodov, Y. Ohara, V. Gusev. Measurement of Nonlinear Ultrasonic Characteristics, chapter 4, Springer (2020).
- [13] V.V. Aleshin, S. Delrue, K. Van Den Abeele, O. Bou Matar. Nonlinear and hysteretic constitutive models for wave propagation in solid media with cracks and contacts. In: *Nonlinear Ultrasonic and Vibro-Acoustical Techniques for*

- Nondestructive Evaluation (Chapter 5), ed. T. Kundu, Springer, Cham, (2019).
- [14] J. Jäger, Axisymmetric bodies of equal material in contact under torsion or shift, *Archive of Applied Mechanics* 65, 478–487 (1995)
- [15] S. Biwa, S. Nakajima, N. Ohno, On the acoustic nonlinearity of solid-solid contact with pressure-dependent interface stiffness, *Journal of Applied Mechanics* 71(4), 508–515 (2004).
- [16] I. Sneddon, *Fourier Series*, Routledge & Kegan, New York (1951).